

Received January 30, 2019, accepted March 4, 2019, date of publication March 7, 2019, date of current version March 26, 2019.

Digital Object Identifier 10.1109/ACCESS.2019.2903599

Recurrent Neural Network-Based Approach for Sparse Geomagnetic Data Interpolation and Reconstruction

HUAN LIU^{1,2,3,4}, (Member, IEEE), ZHENG LIU⁴, (Senior Member, IEEE), HAOBIN DONG^{1,2,3}, JIAN GE^{1,2,3}, ZHIWEN YUAN³, JUN ZHU³, HAIYANG ZHANG³, AND XUMING ZENG⁵

¹School of Automation, China University of Geosciences, Wuhan 430074, China

²Hubei Key Laboratory of Advanced Control and Intelligent Automation for Complex Systems, Wuhan 430074, China

³Science and Technology on Near Surface Detection Laboratory, Jiangsu, Wuxi 214035, China

⁴Faculty of Applied Science, School of Engineering, The University of British Columbia, Okanagan Campus, Kelowna, BC V1V 1V7, Canada

⁵School of Navigation, Wuhan University of Technology, Wuhan 430074, China

Corresponding authors: Jun Zhu (zhujun0506@126.com) and Xuming Zeng (zengxuming@whut.edu.cn)

This work was supported in part by the National Natural Science Foundation of China under Grant 41874212, in part by the Foundation of National Key R&D Program of China under Grant 2018YFC1503702, in part by the Foundation of the Qingdao National Laboratory for Marine Science and Technology under Grant QNLM2016ORP0201, in part by the National Key Scientific Instrument and Equipment Development Project of China under Grant 2014YQ100817, in part by the Foundation of Science and Technology on Near-Surface Detection Laboratory under Grant 6142414180913, Grant TCGZ2016A005, Grant 614241409040218, and Grant 614241409041217, and in part by the Chinese Postdoctoral Science Foundation under Grant 2016M592410.

ABSTRACT Aimed to interpolate the geomagnetic data from under-sampled or missing traces, this paper presented an approach based on recurrent neural network (RNN) techniques to avoid the time & labor-intensive nature of the traditional manual and linear interpolation approaches. In this paper, a deep learning algorithm, long short-term memory (LSTM) was employed to build the precisely model for sparse geomagnetic data interpolation. First, a continuous regression hyperplane was specified to recognize the probably intrinsic relationships between sparse and integral traces by inputting the training data. Afterward, the trained model was tested with 20% of the trained geomagnetic data and other new untrained data for validation. Finally, extensive experiments were conducted for 2D and 3D field data. The results demonstrated that our RNN-based approach was more superior than a classic linear method and a state-of-the-art method, support vector machine (SVM), as the interpolation precision was approximately improved by 10%.

INDEX TERMS Interpolation, geomagnetic data, deep neural network, long short-term memory, modeling

I. INTRODUCTION

The observations of the Earth's magnetic field are implemented continuously spans from a few seconds to decades [1]. However, the integrity of geomagnetic data could not be ensured all the time, especially when equipment failures happen during the acquisitions [2]. In this case, the missing traces or under-sampled data could influence the interpretation result of the geomagnetic data [3], and thus the research on the interpolation and reconstruction for the sparse geomagnetic data is necessitated.

Nowadays, numerous methods for sparse geomagnetic data interpolation were proposed. In terms of simulations, two data assimilation based techniques to forecast the geomagnetic data periods was investigated in literatures [4], [5],

whose results were inspiring. However, these methods had not been adopted in practical scenarios and thus, their effectiveness needs to be further identified. There are a few methods available to real applications, such as the global magnetic field models built in [6] and [7], and the baseline forecasting models for observation and evaluation of the unknown geomagnetic field periods [8]. Further, there are some other commonly used algorithms being investigated such as multi-model fusion [9] and spherical harmonic model [10]. Nonetheless, some drawbacks still exist including that certain assumptions dependence, a limited amount of regression parameters should be comprised in the geomagnetic data observations, the number of the under-sampled data should be less than the obtained data, etc. Aimed to overcome these disadvantages, a new intelligent interpolation method based on support vector machine (SVM) was designed [11]. The results were encouraging, however, it also has drawbacks

The associate editor coordinating the review of this manuscript and approving it for publication was Zhanyu Ma.

in reflecting temporal dependence because of the time and spatial characteristics have not been considered for the interpolation of sparse geomagnetic data.

In this paper, we introduce a new recurrent neural network (RNN) based approach for interpolating geomagnetic data with missing traces due to under-sampling. The proposed RNN-based approach mainly consists of the following three steps: 1) build dataset including the potential relation between input features with missing traces and output ground truth with completed traces. Furthermore, the dataset is split into three clusters including training, testing, and validation data; 2) train probabilistic regression models to fit a potential hyperplane with a continuous regression property from the training data; 3) use the trained model to interpolate the missing geomagnetic traces for validation and testing data. The performance of the proposed RNN-based method only determined by the characteristics of the input training data with intrinsic features, which can overcome the aforementioned drawbacks including the sparsity of missing traces, the assumptions of regression parameters, etc. Consequently, it can not only break through the unsolved problems but also show superior adaptability for different 2D and 3D datasets, which can reduce costs significantly in engineering applications. Furthermore, our method can reduce the manual workload dramatically, for instance, the users do not have to select the window size parameters. It could accelerate engineers to obtain the integral information of Earth’s magnetic field for near-surface exploration, magnetic target detection, etc. Numerical experiments implemented on various field geomagnetic data demonstrate the competitive and applicable performance of our method.

II. METHODOLOGY

The main procedure for sparse geomagnetic data interpolation and reconstruction including three modules: 1) Database building module, which is used to transform the collected 3D or 2D time series geomagnetic data to a 1D space vector; 2) RNN regression module, which is utilized for generating long and short memory cells to build a feed-forward neural network; 3) Interpolation module, which is obtained by constantly optimizing the trained model until it is accuracy in most instances.

A. CONVERTING 3D OR 2D GEOMAGNETIC DATA TO 1D SEQUENCES

For using RNN-based regression model for sparse geomagnetic data interpolation, a regulation to form the collected data into a database consists of the feature x and the ground truth y , which should be suitable for feeding into the training model is necessary. Technically, for a 2D dataset, i.e., the input variables $x = (B_1, B_2, \dots, B_t)$ in which the values are the strengths of magnetic field, and t stands for the collected data in chronological order. Hence, the x could be directly transformed into a 1D vector as $[B_1, B_2, \dots, B_t]^T$.

The procedure for building the database for a 3D dataset is different from that of 2D because all the locations of the

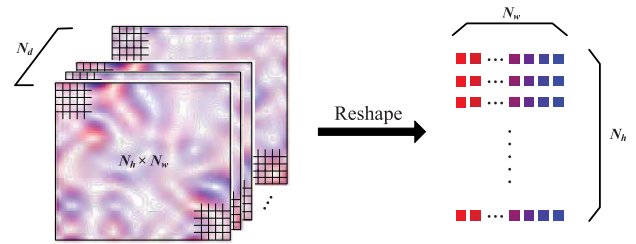


FIGURE 1. The procedure of reshaping 3D time series data into 1D time series data.

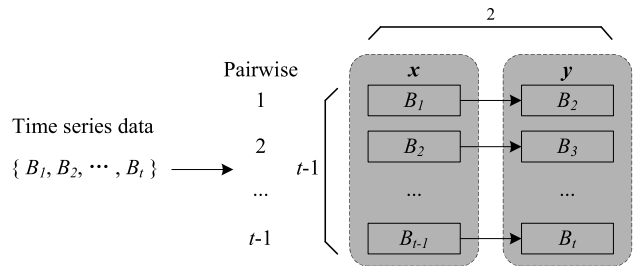


FIGURE 2. The procedure of converting 1D time series data into a data matrix. The feature x stands for the value (refer to B_t) of magnetic field at a given time (t) and ground truth y is the value (refer to B_{t+1}) of magnetic field at the next time ($t + 1$).

3D data sources are described by two spatial dimensions. The procedure of establishing the database for 3D geomagnetic data is shown in Fig. 1. In this case, first, the 3D sequential data is reshaped into 2D array data and thus, the preprocessed data could be seen as an image that each strength value of the magnetic field from each position is expressed by the corresponding pixels with time attributes. $N_w \times N_h$ represents the size of the image, while N_h and N_w are the number of pixels along the column and row axis, respectively. N_d stands for the number of 3D geomagnetic images for training. After the reshaping process, the original time series geomagnetic data, which is transformed into a number array that is converted into a dataset-matrix following the database building steps of 2D. Hence, each sample of reshaped data stands for an combination of pixels from original data along the timeline and thus, the number of samples could be obtained through multiplying the height by the width of the image. As a consequence, we can get $N_w \times N_h \times N_d$ ($100 \times 100 \times 20$) pairwise samples as the feeding dataset to train.

Through the aforementioned preprocessing, the original 2D or 3D time series geomagnetic data is converted into a dataset-matrix as shown in Fig. 2. $(t - 1) \times 2$ represents the size along the timeline, while $(t - 1)$ and 2 are the number of variables along the row and column axis, respectively. In this case, each sample of the pairwise data is a 1D vector, which is a suitable data form for feeding into the RNN-based interpolation model.

B. RNN-BASED INTERPOLATION MODELING

RNN is developed to deal with sequential dependence and consists of an effective neural network structure. It is also

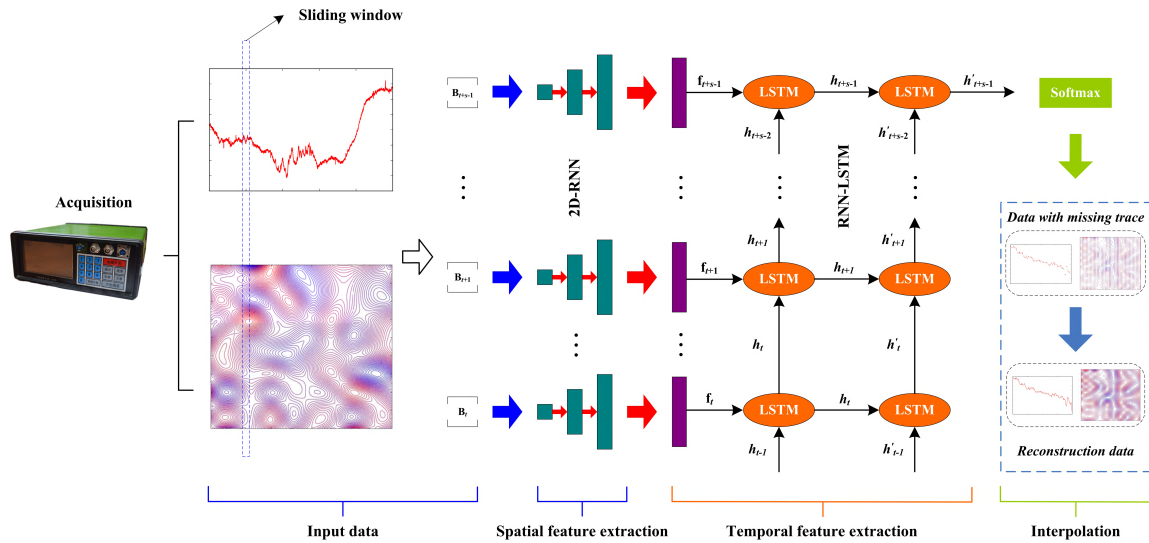


FIGURE 3. The pipeline of proposed RNN-based sparse geomagnetic data interpolation framework.

the extension of feed-forward neural networks, which add a feedback connection [12]. This kind of feedback connection can feed the outputs of the model back into itself, and it has the memorization ability [13].

In this study, the geomagnetic data interpolation model represents a deep RNN framework illustrated in Fig. 3, capturing the spatial and temporal features in sequence. Further, the sliding window technique is applied to divide the pre-processed training data into individual clips. Each clip has a fixed length of time series 1D data, in which the segment S_i is created as follows:

$$S_i = [B_t, B_{t+1}, \dots, B_{t+s-1}] \quad (1)$$

where s is the size of the window and $i = 1, 2, \dots, n$ with n segments through the period of geomagnetic observation. The segment S_j is the input to the model, creating a 3D data architecture containing geomagnetic, spatial and temporal information. We first extract the spatial features, and thus feed the sequence of the extracted spatial features into the RNN to extract temporal features. One fully connected layer receives the output of the last time step of the RNN layers, and feeds the softmax layer for final intention prediction.

The i th input segment is defined as Eq. 1 where there are S data sequences denoted as $B_k = [B_k, B_{k+1}, \dots, B_{k+s-1}]$, where $k = t, t + 1, \dots, t + s - 1$. The sequences are input to a 2D-RNN individually, and each resolves to a spatial feature represent f_k :

$$f_k = RNN_{2D}(B_k) \quad (2)$$

The final spatial feature representation f_k is a feature vector. Through the 2D-RNN spatial feature extraction step, the input segments are transformed to sequences of spatial feature as: $S_i \Rightarrow F_i$, where $F_i = [f_i, f_{i+1}, \dots, f_{i+s-1}]$. Hence, the spatial feature representation sequence F_i is input to a RNN to computes the temporal features.

Further, we use Long Short-Term Memory (LSTM) units to establish two iterative RNN layers. The LSTM is a modified RNN cell addressing the gradient vanishing and exploding problem [14]. The number of each layer's LSTM units is S , and the output time sequence from the previous RNN layer is input to the present RNN layer. At the first RNN layer, the hidden state of the LSTM unit at current time t is indicated as h_t , while the h_{t-1} stands for the hidden state at previous time ($t - 1$). Hence, the information from h_{t-1} is conveyed to h_t , which could determine the final output performance. In this case, the hidden state is regarded as the output of the LSTM unit, and the hidden state sequence of the first RNN layer $[h_t, h_{t+1}, \dots, h_{t+s-1}]$ is the input sequence of the second RNN layer. Thus, the temporal feature representation h'_{t+s-1} of the segment S_i can be written as:

$$h'_{t+s-1} = RNN_{lstm}(F_i) \quad (3)$$

On the right of the fully connected layer is the final softmax layer yielding the final probability predictions of geomagnetic data missing traces as:

$$P_i = Softmax(h'_{t+s-1}) \quad (4)$$

The main steps using RNN-based interpolation model are given in Alg. 1, where the number of LSTM blocks in each of the hidden layers is 10, and the input visible layer is set as 1. The predictions from the output RNN layer is conducted according to the look back who is set as 10. In addition, the number of overall times for the training vectors is 100 (refer to epochs).

C. MISSING TRACES RECONSTRUCTION

Once all the processes mentioned before have been implemented successfully, the output softmax that regarded as an associative function $f(x)$ of the RNN-based interpolation

Algorithm 1 Interpolation Based on LSTM

Result: Sparse geomagnetic data interpolation.
Input : Sparse geomagnetic data x and corresponding ground truth y .
Output: Reconstructed geomagnetic data.

- 1 **Training:**
- 2 A dataset consists of x and y is established, in which x and y denote the magnetic field strength at time (t) and time ($t + 1$), respectively;
- 3 A LSTM based neural network is built as:
- 4 $model = Sequential()$
- 5 $model.add(LSTM(10, input_shape = (1, 10)))$
- 6 $model.fit(x, y, epochs = 100)$
- 7 Fit all pairs of (x_t, x_{t+1}) to the network, which is trained for a $epochs$ of 100.
- 8 **Testing:**
- 9 Input the sparse geomagnetic data x to the established LSTM based neural network to interpolate and reconstruct the missing traces y' ;

model could be yielded. In real scenarios, the interpolation and reconstruction procedures are as follow:

- *Step 1:* Given a sparse geomagnetic data x^* who is never trained before. To some extent, the magnetic field strength x_t^* at time (t) is not available while x_{t-i}^* is known, where $i = (1, 2, \dots)$ is no more than t ;
- *Step 2:* Input x_{t-i}^* to the derived function of the trained LSTM model, and we can obtain $x_{t-i+1}^* = f(x_{t-i}^*)$;
- *Step 3:* Input the yielded value x_{t-i+1}^* to further get $x_{t-i+2}^* = f(x_{t-i+1}^*)$;
- *Step 4:* Repeat step 2) and 3) until x_t^* is calculated by $x_t^* = f(x_{t-1}^*)$.

III. EXPERIMENTAL RESULTS AND ANALYSIS

A. PERFORMANCE EVALUATION METRICS

The proposed RNN-based approach for the interpolation and reconstruction of under-sampled geomagnetic data mainly including the following steps: 1) Building dataset; 2) Training LSTM neural network; 3) Interpolating and reconstruction the sparse geomagnetic data; 4) Validating the model with new untrained dataset. For all the experimental results, the root mean square error (RMSE) and R^2 [15] were employed to evaluate the performance using different algorithms. Their expressions can be written as follow [16]:

$$\left\{ \begin{aligned} RMSE &= \sqrt{\frac{1}{n} \sum_{i=1}^n (y_i - \hat{y}_i)^2} \\ R^2 &= 1 - \frac{\sum_{i=1}^n (y_i - \hat{y}_i)^2}{\sum_{i=1}^n (y_i - \bar{y}_i)^2} \end{aligned} \right. \quad (5)$$

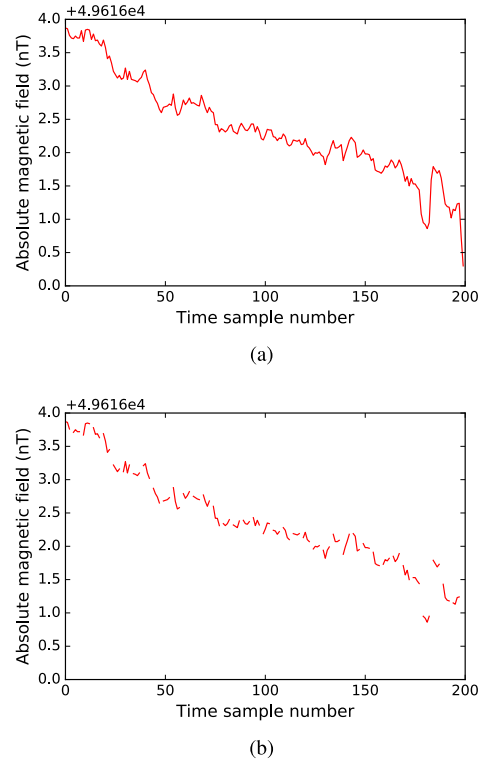


FIGURE 4. 2D Field geomagnetic data for the test. (a) Original 2D field geomagnetic data. (b) Decimated 2D data with 30% regular missing traces.

where y_i stands for the real magnetic field, \hat{y}_i stands for the interpolated magnetic field and \bar{y}_i stands for the value by averaging all the interpolations. RMSE is an absolute measure of fitting while R^2 is a relative measure of fitting. The lower the RMSE, the better the performance. For R^2 , it changes in the range of $0 \sim 1$, and the higher the R^2 , the more superior the model.

B. 2D FIELD GEOMAGNETIC DATA INTERPOLATION

To identify the superiority of the proposed RNN-based algorithm, we used a commercial magnetometer to record the geomagnetic field strength in the field for 24 hours. Fig. 4(a) shows a subset of the collected 2D integral field geomagnetic data. In this case, we compared our new method with a commonly used method, linear interpolation, and a state-of-the-art method, SVM, in a case of 30% regular missing traces as shown in Fig. 4(b).

Fig. 5 shows the interpolation results of the 2D geomagnetic data from Fig. 4(b). Through comparing the reconstructed accuracy using classic linear, SVM and LSTM methods, it can be demonstrated that our new RNN-based approach had a slightly superiority over the commonly used linear and SVM methods. The interpolated data followed approximately the same trend as the recorded geomagnetic field in all cases.

To evaluate the interpolation quality of the results in a more convincing way, the RMSE and R^2 of different algorithm were quantified in Table. 1, where the best and worst results

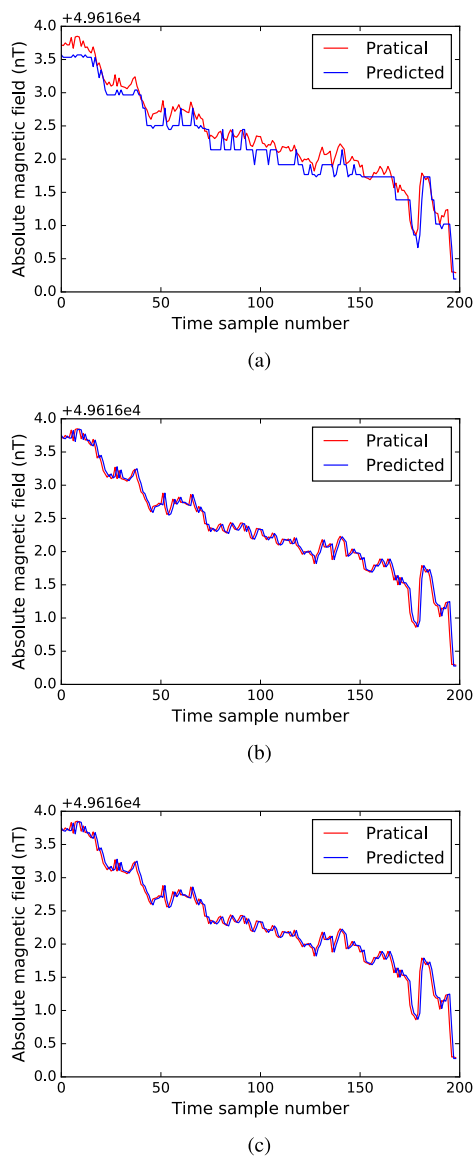


FIGURE 5. The 2D field geomagnetic data interpolation results of different methods. (a) Linear for 2D data interpolation. (b) SVM for 2D data interpolation. (c) LSTM for 2D data interpolation.

were both highlighted in bold font. Among these three methods, LSTM got the best quality of training, validation and testing data sets. The R^2 , RMSE and cross-validation all gave better results, in which the cross-validation was adopted to eliminate the overfitting problem.

C. 3D FIELD GEOMAGNETIC DATA INTERPOLATION

Aimed to further demonstrate the interpolative and reconstructive capacity of our new method, a series of experiments were implemented on 3D field geomagnetic data sets. In this case, different scenarios of the recording region were chosen to guarantee the stochastic and diversity of the data. The width and length of the measurement region were both 10 m and the step over distance was 0.1 m, which implies 100 data should be recorded in each region. Fig. 6(a) shows a 3D integral field

TABLE 1. Comparisons using different methods for 2D and 3D examples.

Method	Dataset	R^2 (2D)	RMSE (2D)	R^2 (3D)	RMSE (3D)
Linear	Testing	0.788	0.279	0.778	0.283
	Training	0.899	0.188	0.903	0.179
SVM	Validation	0.889	0.198	0.895	0.190
	Testing	0.878	0.208	0.887	0.201
LSTM	Training	0.988	0.094	0.972	0.124
	Validation	0.983	0.108	0.965	0.143
	Testing	0.978	0.122	0.958	0.162

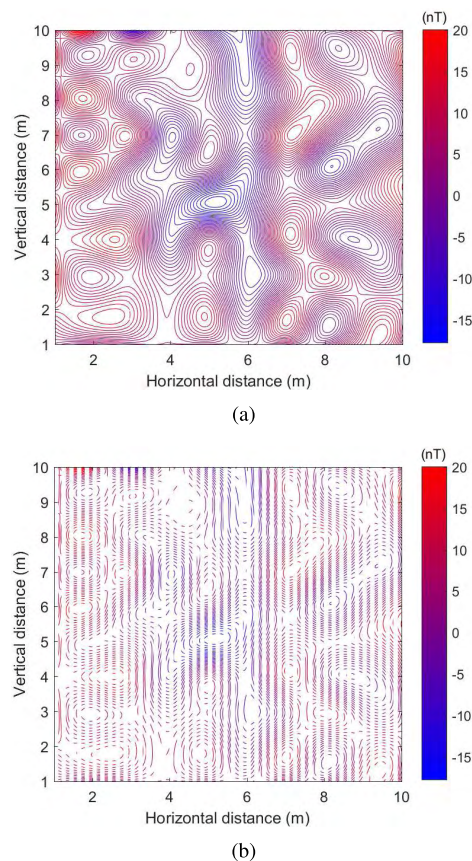


FIGURE 6. 3D Field geomagnetic data for the test. (a) Original 3D field geomagnetic data. (b) Decimated 3D data with 50% regular missing traces.

geomagnetic data. The geomagnetic data have been down-sampled with a regular 50% missing traces, which is shown in Fig. 6(b).

Fig. 7 shows the interpolation results and their trace comparison obtained using linear, SVM and LSTM methods. Overall, our proposed RNN-based approach was also superior than the linear regression method, especially in the region around coordinate (7, 6). In view of the SVM method, the interpolations were also not accurate in each corresponding missing trace, such as the region around coordinate (4, 7) in Fig. 7(b). The reason why these interpolated errors happened might be because of the different characteristics of each model. Nevertheless, the interpolated deviations using the linear method were larger than others, while the interpolations using LSTM were almost the same as the recorded data as shown in Fig. 6(a).

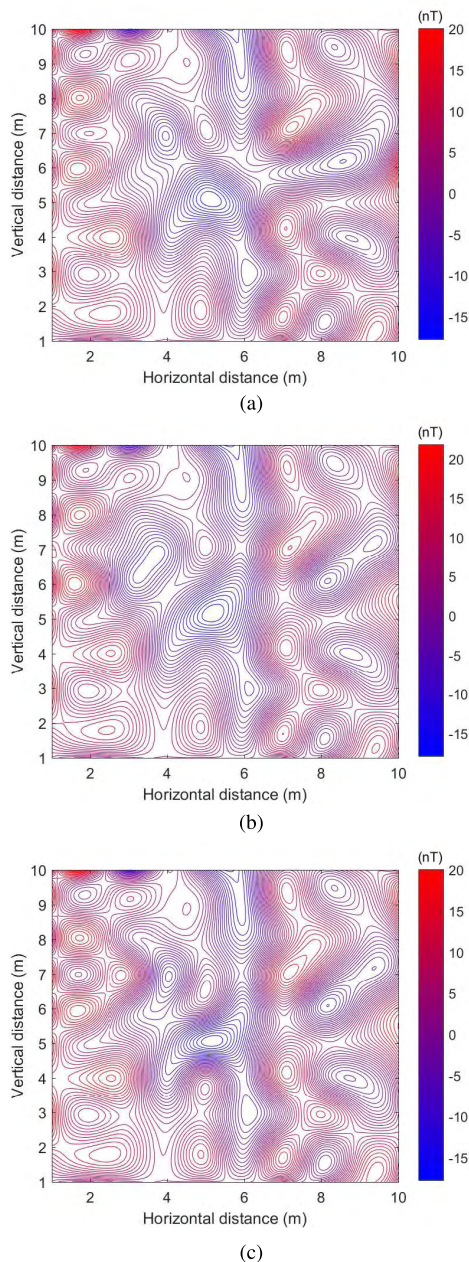


FIGURE 7. The 3D field geomagnetic data interpolation results of different methods. (a) Linear for 3D data interpolation. (b) SVM for 3D data interpolation. (c) LSTM for 3D data interpolation.

Table 1 shows the comparison for linear, SVM and the proposed RNN-based approach in quantitative terms. Again, LSTM got the best performance with training, validation and testing data sets, which were consistent with the results of 2D and 3D examples. Due to the proportional of the under-sampled data in 3D data was larger, the 3D interpolations were worse than that of the 2D example overall. However, it verified better performance significantly through using LSTM method compared with linear regression and SVM methods. Furthermore, our method can handle interpolation problems of practical geomagnetic field data more intelligently without setting complex parameters.

D. DISCUSSION

This paper adopted deep learning method, which could make the training process more complex. Hence, how's the time cost of the whole algorithm is the critical factor that engineers care about most. We followed the main idea that using RNN-based approach for interpolating and reconstructing the sparse geomagnetic data. They were conducted respectively and compared in terms of time cost and accuracy. Time-wise, the running time for the LSTM model is about 913.94 ± 74.32 s while that of SVM model is about 46.02 ± 1.15 s in the training procedure. They also differ in terms of accuracy as shown in Table. 1, and it is up to user to choose which algorithm to use. When we use any one of the algorithms in applications, say given a new set of data, we can use the regression model that was trained using the old data. That means once the model training has been finished and saved, the model could be regarded as a ready-to go instrument, which can be applied directly without training again.

IV. CONCLUSIONS

We proposed an RNN-based method for sparse geomagnetic data interpolation and reconstruction. A intrinsic relation can be obtained using sufficient typical training data sets, from which the missing traces can also be supplemented. Besides, our new RNN-based approach can overcome unsolved drawbacks in existing interpolation methods, and it is universally applicable to varying data sets. Furthermore, the derived interpolation model can be saved for future application, to interpolate the sparse geomagnetic data with different geomorphological structures. To sum up, the experimental results demonstrated that our new method can achieve an interpolation precision no less than 90%, which showed an improvement by about 10% compared to conventional methods, linear regression, and a state-of-the-art method, SVM. Thereby making up for the insufficiency of the reconstruction performance.

ACKNOWLEDGMENTS

The authors are grateful to the editors and anonymous reviewers for their constructive comments to improve this paper.

REFERENCES

- [1] A. Greve, M. J. Hill, G. M. Turner, and A. Nilsson, "The geomagnetic field intensity in new zealand: Palaeointensities from holocene lava flows of the tongariro volcanic centre," *Geophys. J. Int.*, vol. 211, no. 2, pp. 836–852, 2017.
- [2] H. Dong, H. Liu, J. Ge, Z. Yuan, and Z. Zhao, "A high-precision frequency measurement algorithm for FID signal of proton magnetometer," *IEEE Trans. Instrum. Meas.*, vol. 65, no. 4, pp. 898–904, Apr. 2016.
- [3] L. J. L. Pick and M. Korte, "An annual proxy for the geomagnetic signal of magnetospheric currents on Earth based on observatory data from 1900–2010," *Geophys. J. Int.*, vol. 211, no. 2, pp. 1245–1258, 2017.
- [4] F. Lhuillier, J. Aubert, and G. Hulot, "Earth's dynamo limit of predictability controlled by magnetic dissipation," *Geophys. J. Int.*, vol. 186, no. 2, pp. 492–508, 2011.
- [5] G. Hulot, F. Lhuillier, and J. Aubert, "Earth's dynamo limit of predictability," *Geophys. Res. Lett.*, vol. 37, no. 6, 2010, Art. no. L06305.
- [6] M. Dumberry and C. C. Finlay, "Eastward and westward drift of the Earth's magnetic field for the last three millennia," *Earth Planet. Sci. Lett.*, vol. 254, nos. 1–2, pp. 146–157, 2007.

[7] I. Wardinski and M. Korte, "The evolution of the core-surface flow over the last seven thousands years," *J. Geophys. Res., Solid Earth*, vol. 113, no. B5, 2008, Art. no. B05101.

[8] M. Korte, C. Constable, F. Donadini, and R. Holme, "Reconstructing the Holocene geomagnetic field," *Earth Planet. Sci. Lett.*, vol. 312, no. 3, pp. 497–505, 2011.

[9] L. Kapper, F. Donadini, V. Serneels, E. Tema, A. Goguitchaichvili, and J. J. Morales, "Reconstructing the geomagnetic field in west Africa: First absolute intensity results from Burkina Faso," *Sci. Rep.*, vol. 7, Mar. 2017, Art. no. 45225.

[10] A. Nilsson, R. Holme, M. Korte, N. Suttie, and M. Hill, "Reconstructing holocene geomagnetic field variation: New methods, models and implications," *Geophys. J. Int.*, vol. 198, no. 1, pp. 229–248, 2014.

[11] H. Liu et al., "A nonlinear regression application via machine learning techniques for geomagnetic data reconstruction processing," *IEEE Trans. Geosci. Remote Sens.*, vol. 57, no. 1, pp. 128–140, Jan. 2019.

[12] K. Cho et al. (2014). "Learning phrase representations using RNN encoder-decoder for statistical machine translation." [Online]. Available: <https://arxiv.org/abs/1406.1078>

[13] X. Liu, Z. Liu, G. Wang, Z. Cai, and H. Zhang, "Ensemble transfer learning algorithm," *IEEE Access*, vol. 6, pp. 2389–2396, 2017.

[14] A. Graves and J. Schmidhuber, "Framewise phoneme classification with bidirectional LSTM and other neural network architectures," *Neural Netw.*, vol. 18, no. 5, pp. 602–610, 2005.

[15] K. Wagstaff. (2012). "Machine learning that matters." [Online]. Available: <https://arxiv.org/abs/1206.4656>

[16] H. Liu, S. Liu, Z. Liu, N. Mrad, and H. Dong, "Prognostics of damage growth in composite materials using machine learning techniques," in *Proc. IEEE Int. Conf. Ind. Technol. (ICIT)*, Mar. 2017, pp. 1042–1047.



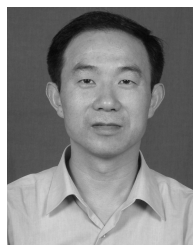
HUAN LIU (S'15–M'18) received the Ph.D. degree in geodetection and information technology from the Institute of Geophysics and Geomatics, China University of Geosciences, Wuhan, China, in 2018, where he is currently an Associate Professor with the School of Automation. From 2016 to 2017, he was a joint training Ph.D. student with Department of Electrical Engineering and Computer Science, School of Engineering, University of British Columbia, Kelowna, Canada.

He has been involved in developing intelligent geophysical instruments, especially, the proton magnetometer and the Overhauser magnetometer. His current research interests include weak magnetic detection, signal processing, data mining, and machine learning.

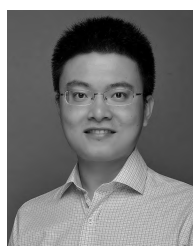


ZHENG LIU (S'99–M'02–SM'06) received the Ph.D. degree in engineering from Kyoto University, Kyoto, Japan, in 2000, and the Ph.D. degree from the University of Ottawa, Canada, in 2007. From 2000 to 2001, he was a Research Fellow with Nanyang Technological University, Singapore. He then joined the Institute for Aerospace Research (IAR), National Research Council Canada, Ottawa, ON, Canada, as a Governmental Laboratory Visiting Fellow nominated

by NSERC. After being with IAR for five years, he transferred to the NRC Institute for Research in Construction, where he was a Research Officer. From 2012 to 2015, he was a Full Professor with the Toyota Technological Institute, Nagoya, Japan. He is currently with the School of Engineering, The University of British Columbia, Okanagan. His research interests include image/data fusion, computer vision, pattern recognition, sensor/sensor networks, condition-based maintenance, and non-destructive inspection and evaluation. He is a member of SPIE. He is chairing the IEEE IMS Technical Committee on industrial inspection (TC-36). He holds a Professional Engineer license in British Columbia and Ontario. He serves on the Editorial Board for journals: the IEEE TRANSACTIONS ON INSTRUMENTATION AND MEASUREMENT, the IEEE Instrumentation and Measurement Magazine, the IEEE JOURNAL OF RFID, Information Fusion, Machine Vision and Applications, and Intelligent Industrial Systems.



HAOBIN DONG received the Ph.D. degree from the Huazhong University of Science and Technology, Wuhan, China, in 2002. He was a Visiting Associate Professor with the Well Logging Laboratory and Subsurface Sensing Laboratory, Department of Electrical and Computer Engineering, University of Houston, Texas, USA, from 2005 to 2006. He is currently a Professor with the School of Automation, China University of Geosciences, Wuhan. His current research interests include weak signal detection and intelligent geophysical instrument.



JIAN GE received the Ph.D. degree in geodetection and information technology from the China University of Geosciences, Wuhan, China, in 2014. He has developed land and marine proton precession magnetic sensor based on polarization and dynamic nuclear polarization effect. He is currently an Associate Professor with the School of Automation, China University of Geosciences. His current research interests include weak signal detection, geophysical detection methods, and instruments.

ZHIWEN YUAN is currently a Senior Engineer with the Science and Technology on Near Surface Detection Laboratory, Wuxi, China. His current research interest includes near surface detection technology.

JUN ZHU is currently a Senior Engineer with the Science and Technology on Near Surface Detection Laboratory, Wuxi, China. His current research interest includes near surface detection technology.

HAIYANG ZHANG is currently a Senior Engineer with the Science and Technology on Near Surface Detection Laboratory, Wuxi, China. His current research interest includes near surface detection technology.



XUMING ZENG received the Ph.D. degree in geodetection and information technology from the Institute of Geophysics and Geomatics, China University of Geosciences, Wuhan, China, in 2018. From 2016 to 2017, he was a joint training Ph.D. student with Electrical and Computer Engineering, College of Engineering, Florida State University, Tallahassee, FL, USA. He holds a postdoctorate position with the School of Navigation, Wuhan University of Technology, Wuhan. His current research interests include routing protocols, MAC, QoS, clustering, radio resource management, traffic engineering, and performance analysis, for both wired and wireless networks.

...